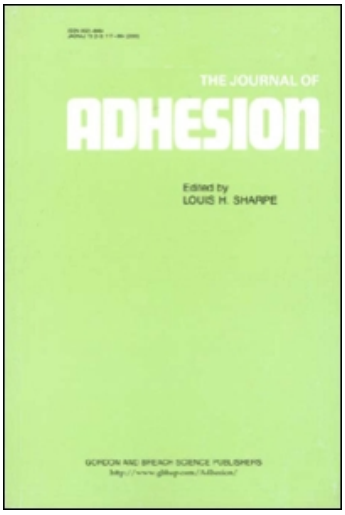

The Journal of Adhesion
Publication details, including instructions for authors and subscription information:
http://www.informaworld.com/smpp/title~content=t713453635

Comparison between the adherence of a rigid axisymmetrical cone and a truncated one, in adhesive contact on an elastic half-space

Michel Barquins[a]
[a] Laboratoire de Physique et de Mécanique des Milieux Hétérogènes, ESPCI, Paris, France

Online publication date: 08 September 2010

To cite this Article Barquins, Michel(2003) 'Comparison between the adherence of a rigid axisymmetrical cone and a truncated one, in adhesive contact on an elastic half-space', The Journal of Adhesion, 79: 10, 915 — 936
To link to this Article: DOI: 10.1080/714906140
URL: http://dx.doi.org/10.1080/714906140

The Journal of Adhesion, 79: 915–936, 2003

ISSN: 0021-8464 print/1545-5823 online
DOI: 10.1080/00218460390247725

Taylor & Francis
Taylor & Francis Group

COMPARISON BETWEEN THE ADHERENCE OF A RIGID AXISYMMETRICAL CONE AND A TRUNCATED ONE, IN ADHESIVE CONTACT ON AN ELASTIC HALF-SPACE

Michel Barquins
Laboratoire de Physique et de Mécanique des Milieux Hétérogènes, ESPCI, Paris, France

We compare the equilibrium contacts and the kinetics of adherence of an axisymmetrical rigid cone and a flat-ended one with the same angle, applied against the flat and smooth surface of a soft elastomer sample (unfilled vulcanized natural rubber, cured with dicumyl peroxide), with the help of fracture mechanics concepts which can easily be introduced in this class of problems by using Sneddon's solution (1965) of Boussinesq's problem extended to all axisymmetric adhesive punches with a convex profile. The kinetics of adherence are measured when an imposed tensile force is applied in order to disturb the size of the contact area. Variations of the strain energy release rate, G, and of the associated dissipation function $\Phi = (G - w)/w$, where w is the Dupré energy of adhesion, are studied as a function of the parameter, $a_T \cdot V$, in which V is the crack propagation speed at the interface between a cone and a truncated one made of glossy Plexiglass®, and the rubber sample (the limit of the contact is considered as a crack tip), and a_T, is the shift factor of the Williams-Landel-Ferry transformation. As expected, a master curve $\Phi(V)$ is found, confirming the variation of Φ as the power function $V^{0.55}$, at fixed temperature, as recently established by Barquins et al. in adherence of a flat ended sphere and cone in pull-off/push-on tests, adherence and rolling of cylinders experiments and rebound of balls tests, with the same elastomer. Present results lead to propose one to write $\Phi = k \cdot (a_T \cdot V)^{0.55}$, $k = 2520$ and V being valued using S.I. units, for the reference temperature $\theta = 25°C$, with a quite good accuracy in the order of 1%.

Keywords: Natural rubber; PMMA perfect and flat-ended conical punches; Fracture mechanics and nondestructive testing; Adhesion tests and kinetics of adherence

Received 29 April 2003; in final form 3 July 2003.

One of a Collection of papers honoring Jacob Israelachvili, the recipient in February 2003 of *The Adhesion Society Award for Excellence in Adhesion Science, Sponsored by 3M*.

The author thanks Spéphane Bouissou and Denis Vallet for experimental assistance.

Address correspondence to Michel Barquins, Laboratoire de Physique et de Mécanique des Milieux Hétérogènes, ESPCI, 10 rue Vacquelin, F-75231, Paris Cedex 05, France. E-mail: babar@pmmh.espci.fr

INTRODUCTION

An earlier study [1], drawing upon Sneddon's 1965 generalisation of Hertz's problem to all axisymmetrical rigid punches with a convex profile [2], investigated the theoretical conditions of the equilibrium adhesive contact between a cone and the smooth and flat surface of an elastic half-space as a soft natural rubber sample. To take into account the molecular attraction forces of van der Waals type in the case of elastomers, as has been previously demonstrated [3], the constant of integration, $\chi(1)$, appearing in formulae and corresponding to a rigid vertical displacement, is assumed nonzero [1, 9, 13]. Experiments are performed using an unfilled vulcanised natural rubber half-space, cured with dicumyl peroxide (modulus of elasticity $E = 0.89\,\text{MPa}$, Poisson ratio's $\nu = 0.5$ and glass transition temperature $T_g = 201\,\text{K}$), and a rigid transparent cone and a truncated one, optically smooth, made of Plexiglass® (PMMA), with a half-angle $\alpha = \pi/2 - \beta = 85$ degrees (Figures 1 and 2). When the normal applied mass, m, is changed, the equilibrium, which depends on the intensity of van der Waals forces, is disturbed. Such a situation will lead either to a separation of the two bodies or to a new equilibrium, depending on the value of the new applied active mass.

Since 1996, Barquins *et al*. [4–10] have conducted various experiments into adherence kinetics and the adhesive behaviour of several axisymmetrical rigid punches and of cylindrical rollers. Moreover, they have performed rebound tests of rigid balls on smooth natural rubber half-spaces. This research has shown that the dissipation function, Φ, for viscoelastic losses located at the edge of the contact zone, which can be inferred from the strain energy release rate G[11], $\Phi = (G - w)/w$, where w denotes the Dupré adhesion energy, varies over a wide range of propagation speeds as a power function of the crack propagation speed, $\Phi \sim V^{0.55}$.

The main goal of this article is to compare behaviours of a rigid axisymmetrical perfect cone and a truncated one with the same angle, in terms of equilibrium conditions of adhesive contacts against a rubber surface, and the kinetics of separation when a new applied load is imposed. It is also shown that the dissipation function, Φ, remains a power function (0.55) of the variation with time of contact area's radius (crack propagation speed) for the specific type of rubber used (unfilled natural rubber) at fixed temperature, and that this function, Φ, can be written $\Phi = k \cdot (a_T \cdot V)^{0.55}$ with $k = 2520$ and speed V being valued using S.I. units, for the reference temperature $\theta = 25^\circ\text{C}$, with a quite good accuracy in the order of 1%.

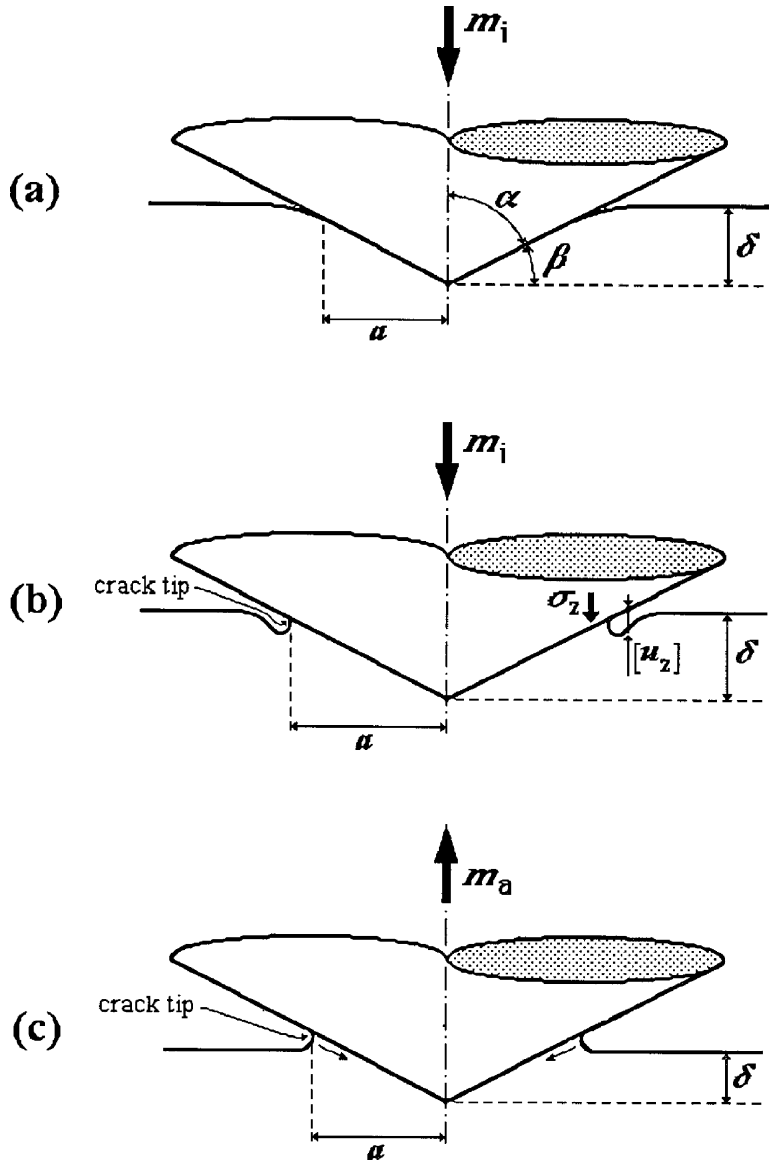

FIGURE 1 Schematic views of the profile between a rigid axisymmetric conical punch and the flat and smooth surface of an elastic half-space: (a) as soon as the mass m_i (corresponding force $P_i = m_i \cdot g$) is applied; (b) at equilibrium under the constant mass m_i; and (c) at the beginning of the detachment when a constant mass m_a smaller than m_i is applied, corresponding to the load $P_a = m_a \cdot g$, which can be less compressive than $P_i = m_i \cdot g$, or to be a tensile force ($P_i = m_a \cdot g < 0$), which leads ineluctably to the rupture of the contact.

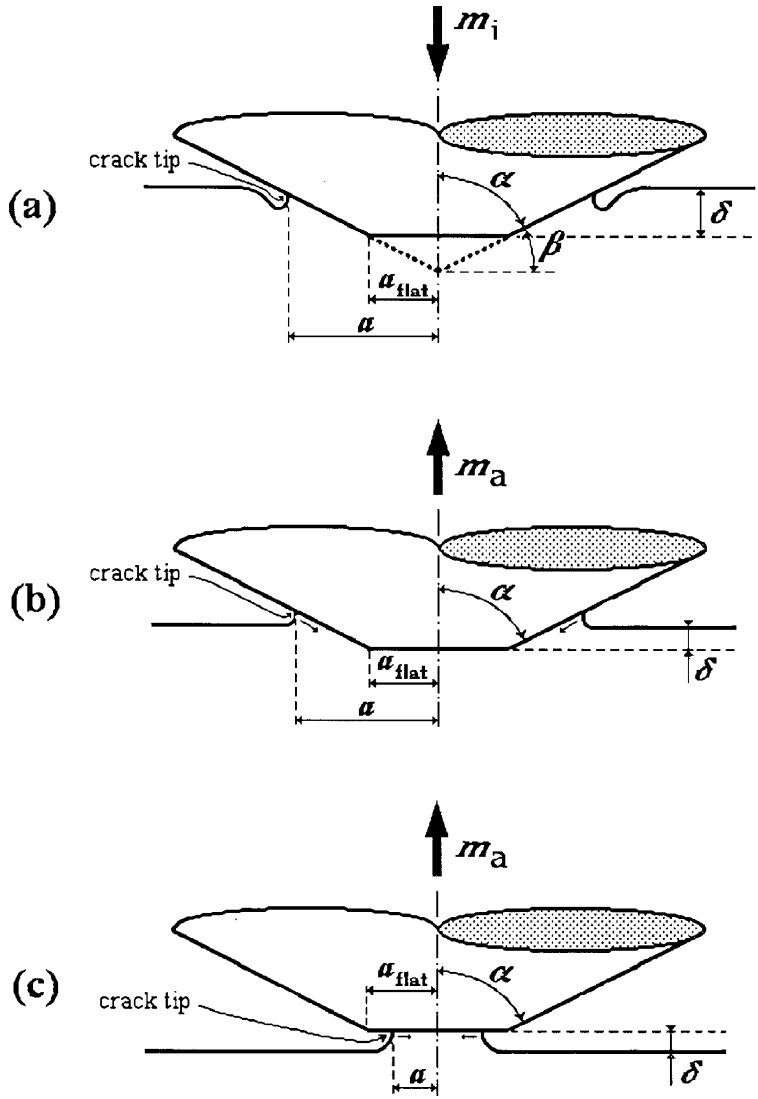

FIGURE 2 Schematic views of the profiles: (a) of the adhesive contact between a flat-ended cone and the flat and smooth surface of an elastic half-space at equilibrium, under the constant compressive mass m_i (profile corresponding to the Figure 1b observed for a perfect conical punch); and (b) of the rubber surface when a tensile mass m_a is imposed, the contact diameter being greater than the flat one and (c) if the contact area is smaller than the flat zone size.

ADHESIVE CONTACT OF AN AXISYMMETRICAL RIGID CONE

Sneddon [2] has derived a solution of the axisymmetric Boussinesq problem from which he deduced simple formulae for the depth of penetration, δ, of the tip of a punch of convex arbitrary profile, for the total load, P, which must be applied to the punch to achieve this penetration, for distribution of pressure, $\sigma_z(r,0)$, under the punch at the distance, r, of the symmetry axis inside the contact area, and for the displacement, $u_z(r,0)$, of the surface at the distance, r, of the contact center outside the contact area. From these formulae [1, 9, 12–13] and from the shape function of a perfect rigid conical punch, given by

$$f(x) = a \cdot x \cdot \tan\beta, \tag{1}$$

where a is the radius of the contact area and x the normalized distance $x = r/a$ from the center of the circular contact, we can deduce the vertical penetration of the perfect rigid cone. Indeed, for all the axisymmetrical punches with continuous and convex profile, Sneddon [2] lets the integration constant $\chi(1) = 0$ in order to have a finite normal stress at the edge of the contact area, and he uses this criterion to determine the penetration, δ. For a conical punch, the classical result is

$$\delta = \frac{\pi}{2} \cdot a \cdot \tan\beta. \tag{2}$$

As demonstrated earlier [3], the hypothesis $\chi(1) = 0$ is not imperative, and the case $\chi(1) \neq 0$ allows one to describe precisely the adhesive contacts of axisymmetrical punches, as a perfect cone or a flat-ended one, in the present case, taking into account the Dupré energy of adhesion, $w = \gamma_1 + \gamma_2 - \gamma_{12}$, of the facing solids (the γ_i and γ_{ij} are the surface and interfacial energies, respectively). It is usual now [3] to consider the parameter K_I:

$$K_I = -\frac{E}{2(1-\nu^2)} \cdot \sqrt{\frac{\pi}{a}} \cdot \chi(1), \tag{3}$$

so that calculations of the stress, σ_z, inside the area of contact near the edge and the discontinuity of displacement $[u_z]$ outside it (Figure 1b) lead to formulae found in fracture mechanics in opening mode (Mode I) and plane deformation, and K_I is the stress intensity factor. They appear because the edge of the contact area can be considered as a crack tip that recedes or advances according to whether the load, P, increases or decreases. In this case, the strain energy release rate, G, is given by

$$G = \frac{1}{2} \cdot \frac{1 - \nu^2}{E} \cdot K_I^2, \tag{4}$$

where E is Young's modulus and ν Poisson's ratio for the elastic half-space. The coefficient (1/2) makes allowance for the fact that the rigid punch undergoes no deformation when applied against the elastic solid.

If P_1 represents the load which gives rise to the same radius of contact area in the absence of molecular attraction force (*i.e.*, $\chi(1) = 0$), and if we denote by P the actual applied load ($P_1 > P$) when these forces do come into play (*i.e.*, $\chi(1) \neq 0$), it can be shown [3] that

$$P_1 - P = -\frac{\pi \cdot E \cdot a}{1 - \nu^2} \cdot \chi(1) = \sqrt{4\pi \cdot a^3} \cdot K_I.$$

Thus the strain energy release rate, G, given by the relation in Equation (4), may be written as

$$G = \frac{1 - \nu^2}{E} \cdot \frac{(P_1 - P)^2}{8\pi \cdot a^3}. \tag{5}$$

As previously demonstrated [13–14], this relation is perfectly universal, which is available for all axisymmetrical punches with convex profile, the load P_1 being only dependent on the shape of the punch and on the elastic properties of the rubber-like material on which this punch is applied.

Taking into account the shape function for a perfect conical punch, it was shown [1, 9, 13] that the vertical displacement is given by

$$\delta = \frac{\pi \cdot a}{2} \cdot \tan\beta - \sqrt{2\pi \cdot a \cdot w \cdot \frac{1 - \nu^2}{E}}, \tag{6}$$

so that the load, P, the radius, of the contact area, a, and the penetration, δ, in the elastic half-space are linked by the relation

$$P = \frac{2E \cdot a}{1 - \nu^2} \cdot \left(\delta - \frac{\pi \cdot a}{4} \cdot \tan\beta\right), \tag{7}$$

which is the state equation of the system.

For an adhesive contact of a rigid axisymmetric conical perfect punch, it is well known [9, 13] that the apparent load, P_1, is equal to

$$P_1 = \frac{\pi \cdot E}{2(1 - \nu^2)} \cdot a^2 \cdot \tan\beta, \tag{8}$$

and it can be verified that the connection of the elastic half-space to the cone is tangential if $\chi(1) = 0$ (Figure 1a), and vertical if $\chi(1) \neq 0$ (geometry of fracture mechanics, as shown on Figures 1b and 1c).

Due to the intervention of molecular attraction forces a finite area of contact exists at equilibrium under zero load, and the value of the corresponding radius, $a_{(P=0)}$, is obtained from Equations (6) and (7):

$$a_{(P=0)} = \frac{1-\nu^2}{2\pi \cdot E} \cdot w \cdot \left(\frac{8}{\tan\beta}\right)^2. \tag{9}$$

Moreover, these molecular attraction forces allow one to apply a tensile force, at equilibrium, whose critical value, P_c, is given [1] by $G = w$ and $(\partial G/\partial A)_p = 0$, A being the contact area ($A = \pi a^2$):

$$P_c = -\frac{54(1-\nu^2) \cdot w^2}{\pi \cdot E \cdot tan^3\beta}. \tag{10}$$

P_c is the quasistatic force of adherence of a perfect cone at fixed load, *i.e.,* the ultimate tensile force that can sustain the conical punch in equilibrium adhesive contact on the elastic half-space.

The radius, a_c, of this ultimate equilibrium contact area can be deduced from Equation (10) with $G = w$, P_1 and $P = P_c$ being given by Equations (8) and (10), respectively:

$$a_c = \frac{18(1-\nu^2) \cdot w}{\pi \cdot E \cdot \tan^2\beta}. \tag{11}$$

Taking into account the value $w = 43\,\text{mJ.m}^{-2}$ (corresponding to experimental data presented in Section 5), the computed value $a_c = 33.5\,\mu\text{m}$ is found.

As already described for adhesive contacts of perfect spherical punches and truncated spheres [7], equilibrium measurements were used in order to verify the value of Young's modulus of the test material, as declared by the elastomer's manufacturer, whereupon a precise value for the Dupré energy of adhesion was obtained. This simple method consists of writing the relation linking the equilibrium contact radius, *a, versus* the normal applied load, P (relation in Equation (7), with δ given by Equation (6)), using Equation (5) in which $G = w$:

$$P = \frac{\pi \cdot E \cdot a^2 \cdot \tan\beta}{2(1-\nu^2)} - \sqrt{\frac{8\pi \cdot a^3 \cdot E \cdot w}{1-\nu^2}}. \tag{12}$$

Dividing all the terms of the relation in Equation (12) by $a^{3/2}$, and assuming that $\nu = 0.5$ for the soft natural rubber tested, we obtain

$$P \cdot a^{-3/2} = \frac{2\pi \cdot E \cdot \tan\beta}{3} \cdot a^{1/2} - \sqrt{\frac{32\pi \cdot E \cdot w}{3}}, \tag{13}$$

from which we conclude that $P \cdot a^{-3/2}$ varies linearly as a function of the square root of the radius, a, of the contact area and, thus, the measurement of the slope allows the calculation of Young's modulus, E. Finally, the determination of the ordinate at the origin furnishes, once E is known, the Dupré energy of adhesion, w.

PARTICULAR CASE OF A FLAT-ENDED CONE

Let us consider the particular case of a rigid transparent truncated cone, optically smooth, made of Plexiglass® (PMMA), with the same half-angle, $\alpha = \pi/2 - \beta = 85$ degrees, as previously, whose circular flat zone (diameter $\varnothing_{\text{flat}} = 2a_{\text{flat}} = 514\,\mu\text{m}$) is parallel to the interface. The particular profile for the adhesive equilibrium contact is schematically shown in Figure 2a, and its transformation when a tensile force is imposed is exhibited in Figures 2b and 2c. The shape function of the punch is now given by [10, 13]

$$f(x) = 0, \quad \text{for } 0 < x < \rho,$$

and

$$f(x) = (x - \rho) \cdot a \cdot \tan\beta, \quad \text{for } x > \rho,$$

where ρ represents the ratio a_{flat}/a.
From Sneddon's equations [1–3, 10, 13], the vertical penetration of the truncated cone is

$$\delta = \frac{1}{2}\pi \cdot \chi(1) + a \cdot \tan\beta \cdot \cos^{-1}\rho, \tag{14}$$

so that the state equation of the system linking the actual applied load, P, to the radius, a, of the contact area and the penetration, δ, in the elastic half-space is given by

$$P = 2E \cdot a \cdot \left[\delta - \frac{a \cdot \tan\beta \cdot (\cos^{-1}\rho - \rho \cdot \sqrt{1-\rho^2})}{2(1-\nu^2)}\right]. \tag{15}$$

Obviously, for $\rho = 0$ (*i.e.*, $a_{\text{flat}} = 0$), Equation (15) reiterates the relationship for an adhesive perfect rigid conical punch (Equation (7)).

Concerning the load, P_1, which gives the same radius of contact when the molecular attraction forces do not act ($\chi(1) = 0$), its value for a truncated cone is given by

$$P_1 = a^2 \cdot \tan\beta \cdot \frac{E}{1-\nu^2} \cdot (\cos^{-1}\rho + \rho \cdot \sqrt{(1-\rho^2)}). \tag{16}$$

This relation in Equation (16) provides $P_1 = 0$ if $\rho = 1$, which exactly corresponds to the contact of a cylindrical punch with a circular cross section [11].

The strain energy release rate is thus

$$G = \frac{(P_1 - P)^2}{8\pi \cdot a^3} \cdot \frac{1 - \nu^2}{E} = \frac{1}{2\pi \cdot a} \cdot \frac{E}{1 - \nu^2} \cdot (\delta - a \cdot \tan \delta \cdot \cos^{-1} \rho)^2. \quad (17)$$

At equilibrium, $G = w$, so that the radius of contact area is linked to the normal applied load, P, by the relation in Equation (5),

$$P = P_1 - \sqrt{\frac{8\pi \cdot a^3 \cdot w \cdot E}{1 - \nu^2}}, \quad (18)$$

the load P_1 being given by the relation in Equation (16). The quasi-static force of adherence of a flat-ended cone at fixed load, P_c, is given, as previously, by $G = w$ and $(\partial G/\partial A)_p = 0$, A being the contact area ($A = \pi a^2$). The corresponding radius of contact, a_{crit}, is provided by the solution of the Equation (17):

$$a_{crit} = \frac{9\pi \cdot w \cdot (1 - \nu^2)}{2E \cdot \tan^2 \beta} \cdot \left(\cos^{-1} \rho_{crit} + \frac{\rho_{crit}}{\sqrt{1 - \rho_{crit}^2}} \right)^{-2}, \quad (19)$$

with $\rho_{crit} = a_{flat}/a_{crit}$.

Obviously, with $\rho_{crit} = 0$ (*i.e.*, $a_{flat} = 0$), the relation in Equation (19) gives the previous one (relation in Equation (11)) for a perfect rigid cone. Taking into account the value $w = 47\,\text{mJ.m}^{-2}$ (corresponding to experimental data presented below), the computed value $\varnothing_{crit} = 2a_{crit} = 514.6\,\mu\text{m}$ is just slightly greater than the size of the flat zone on the truncated cone, $\varnothing_{flat} = 514\,\mu\text{m}$.

KINETICS OF THE ADHERENCE

The adherence kinetics at any equilibrium state ($G = w$) is usually studied by changing the initial applied mass, m. When m is suddenly lowered for a given contact radius, a, *i.e.*, the apparent load, P_1, remains temporarily constant (Equations (14) and (22) for a perfect and a flat-ended cone, respectively), the strain energy release rate, G (Equation (5)), rises so that $G > w$ and the solids begin to separate (Figures 1c and 2b). At the present time, one is quite well aware that the difference $(G - w)$ represents the applied force per unit length of the crack [11]; this is the driving force to the "motor" of the crack, whose speed limit entirely depends on temperature. If we suppose

that the viscoelastic losses are proportional to w and that they are localized at the crack tip [15, 16], we may write

$$G - w \equiv w \cdot \Phi(a_T \cdot V), \tag{20}$$

an identity in which the right-hand term corresponds to the viscous drag resulting from losses within the crack tip. the dimensionless function, $\Phi(a_T \cdot V)$, entirely depends on the crack propagation speed, V, and on the absolute temperature, T, of experiments, through the shift factor, a_T, of the WLF transformation [17]:

$$\log_{10} a_T = \frac{-8.86(T - T_0)}{101.6 + T - T_0}, \tag{21}$$

where T_0 is a temperature of reference defined from the glassy absolute temperature, T_g, of the rubber sample by $T_0 = T_g + 50\,\mathrm{K}$.

At each instant, the crack propagates at such a speed, V, that the corresponding viscoelastic losses precisely offset the shift effect $(G - w)$, and the speed, V, varies if G is modified when the contact radius, a, evolves over time. The function Φ is characteristic of the types of elastomers tested for propagation in Mode I (opening mode), and may be directly related to the frequency dependence of the imaginary component of Young's modulus [18].

As already announced twenty-five years ago, the main interest of the Equation (20) is that surface properties (w) and viscoelastic losses (Φ) are clearly dissociated from the loading conditions and the system geometry which only appear in the rate G. Predictions assume only that (1) the kinetic energy is negligible; (2) the rupture is adhesive, *i.e.*, the propagation occurs at the interface so that experiments at equilibrium ($V = 0$) give the Dupré energy of adhesion, w; and (3) viscous losses are limited to those areas where stress and strain rates are high, which implies that gross displacements are purely elastic and the strain energy release rate, G, can still be calculated by the theory of linear elasticity during crack propagation. Moreover, one should note that the existence of a unique value assumed for the Dupré energy of adhesion, which appears in the Equation (20) as a negative term on the left-hand side and a multiplicative term on the right-hand side, is a natural result from highly crosslinked material, so that hysteresis effects between loading and unloading are not observed.

Starting from the equilibrium state under the mass m_i (the corresponding applied force is $P_i = m_i \cdot g$, where g is the acceleration due to gravity), the study of the kinetics of adherence consists in measuring the evolution over time, t, of the diameter, $\varnothing$, of the contact area

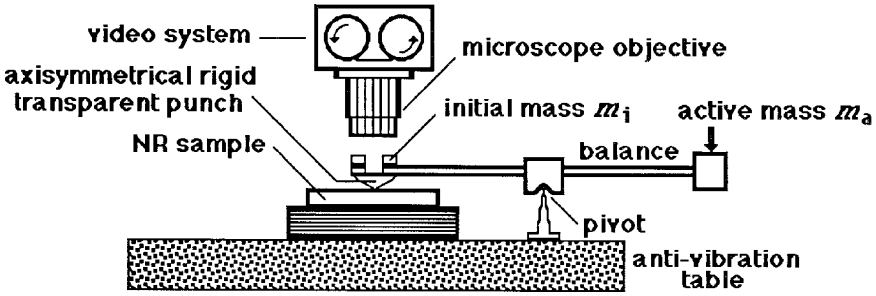

FIGURE 3 Schematic arrangement of the apparatus used at the present time to study equilibrium adhesive contact areas of a rigid axisymmetrical punch, made of transparent material (glossy glass or PMMA), under various applied masses, and the kinetics of adherence when a constant normal mass is imposed in order to lead to a new equilibrium state or to the rupture of the contact area, following its intensity.

when another mass, $m_a < m_i$, is imposed and remained constant. For that, a new mass, M_a, is imposed at the rear part of the balance (right side of Figure 3) so that the mass, $m_a = m_i - M_a$, is now active. For each value of the contact diameter, $\varnothing = 2a$, the strain energy release rate, G, can be calculated with the help of the Equation (5), the load P_1 being given by Equations (8) and (16) for the perfect and the truncated cone, and linked to the crack propagation speed, $V = -(1/2)\mathrm{d}\varnothing/\mathrm{d}t$. Moreover with the determination of w by means of a simple method, which will be described later, we may plot the variation of the dissipation function, Φ, with the help of Equation (20), as a function of the speed, V, and verify the previous results for natural rubber [4–10, 19] in regards to the existence of a master curve representing Φ in terms of speed, V, raised to the power 0.55.

EXPERIMENTAL RESULTS FOR THE PERFECT CONICAL PUNCH AND DISCUSSION

Equilibrium and separation kinetics experiments were carried out at constant temperature $\theta = 26^{\circ}\mathrm{C}$ and relative humidity $RH = 53\%$, between a rigid axisymmetric conical punch made of Plexiglass® (PMMA), with the vertical half-angle, $\beta = 5$ degrees (Figure 1), and the smooth, flat surface of a sheet of soft unfilled vulcanized natural rubber, cured with dicumyl peroxide (Young's modulus $E = 0.89\,\mathrm{MPa}$, Poisson's ratio $\nu = 0.5$ and glass transition temperature $T_g = 201\,\mathrm{K}$),

with a thickness, $e = 6\,\text{mm}$, of sufficient width with respect to the contact areas so as to be considered as an elastic half-space.

To study the equilibrium in a first set of experiments, the perfect conical rigid punch was pressed by a mass, m_i (initial force corresponding to $P_i = m_i \cdot g$), during a constant time, $t_i = 10\,\text{min}$, a duration necessary so that the molecular attraction forces would clearly manifest themselves [20] (the area of contact increases and the surface takes a fracture mechanics profile as schematically shown on Figures 1a and 1b) against the smooth surface of elastomer, by means of an incorporated microscope balance fitted with a video camera to record both the contact areas and their immediate neighbourhood through the transparent conical punch (Figure 3) and their precise measurements afterwards, with an accuracy of the order of $2\,\mu\text{m}$ on contact diameter size. This is accomplished in our usual manner, which was begun twenty-five years ago, using a 16 mm camera providing only 24 frames per second [11] instead of 50 at the present time. To examine the separation kinetics after the time interval, t_i, the initial mass, m_i is removed and various active masses $m_a < m_i$ were applied at the rear part of the balance. The decrease in contact area radius (as shown in Figure 1c with regard to Figure 1b, for example) was recorded during an interval $t_a < 30\,\text{s}$, a duration deliberately very shortened with respect to t_i so as to avoid the dwell time effects [20, 21]. Before contact, rubber sample and conical punch surfaces were cleaned with isopropyl alcohol and left to dry in a dust-free open air environment for 15 min, thus allowing their surfaces to reach an equilibrium with ambient atmosphere.

Figure 4 shows the equilibrium contact diameters, $\varnothing$, between the perfect cone made of transparent Plexiglass® (PMMA) with $\beta = 5$ degrees and the elastomer surface (natural rubber, NR) as a function of the initial mass, m_i. Due to the intervention of molecular attraction forces, of van der Waals type, a finite area of contact exists at zero applied load. Moreover, as well known for spherical indenters, flat punches, flat-ended spheres, and cone, [7, 9–11, 22–24] equilibrium contact areas exist under negative loading, but in the case of a conical punch, unfortunately these tensile loads are very small [1, 9]. As an example, the quasistatic force of adherence of the perfect rigid cone at fixed load, given by the relation in Equation (10), is equal to $P_c = -40\,\mu\text{N}$, with $w = 43\,\text{mJ.m}^{-2}$, a value which cannot be well verified with the help of our experimental apparatus whose sensitivity is of the order of $20\,\mu\text{N}$.

We have used the equilibrium measurements (Figure 4) and Equation (13) to verify the value of Young's modulus for the test material and to obtain a precise value for the Dupré adhesion

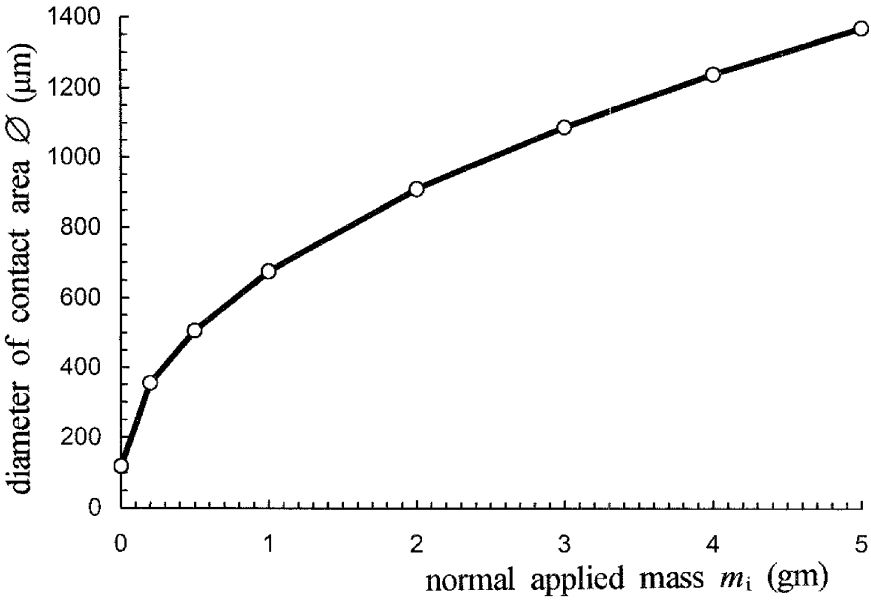

FIGURE 4 Diameters, $\varnothing$, of equilibrium contact areas between the conical rigid punch and the flat and smooth surface of an elastic solid (soft unfilled vulcanized natural rubber, cured with dicumyl peroxide, Young's modulus $E = 0.89\,\text{MPa}$, Poisson's ration $\nu = 0.5$, and glassy transition temperature $T_g = 201\,\text{K}$) as a function of the normal applied mass, m_i. The heavy line joins experimental data. (Reprinted from D. Vallet and M. Barquins, "Adhesive contact and kinetics of adherence of a rigid conical punch on an elastic half-space (natural rubber)," *Int. J. Adhesion and Adhesives* **22**, pp. 41–46, copyright 2002, with permission of Elsevier).

energy. Figure 5 shows the variation of the parameter $P \cdot a^{-3/2}$ as a function of $a^{1/2}$. The linear regression gives the slope $s = (2/3)\pi E \cdot \tan\beta = 147955\,\text{Pa}$, from which can be deduced the value of Young's modulus $E = 897231\,\text{Pa}$, which corresponds very well (with an accuracy better than 1%) to the value declared by the elastomer's manufacturer ($E = 0.89\,\text{MPa}$). The value at the y axis at the origin $-\sqrt{(32/3)\pi \cdot E \cdot w} = -1142\,\text{N.m}^{-3/2}$ furnishes, once E is known, the Dupré energy of adhesion, $w = 43\,\text{mJ.m}^{-2}$. This value is slightly smaller than the previous one [6, 7, 19] due to a small increase in the relative humidity, which is highest in the present experiments. It is well demonstrated in peeling experiments that an increase in relative humidity, RH, decreases the Dupré energy of adhesion, w [24].

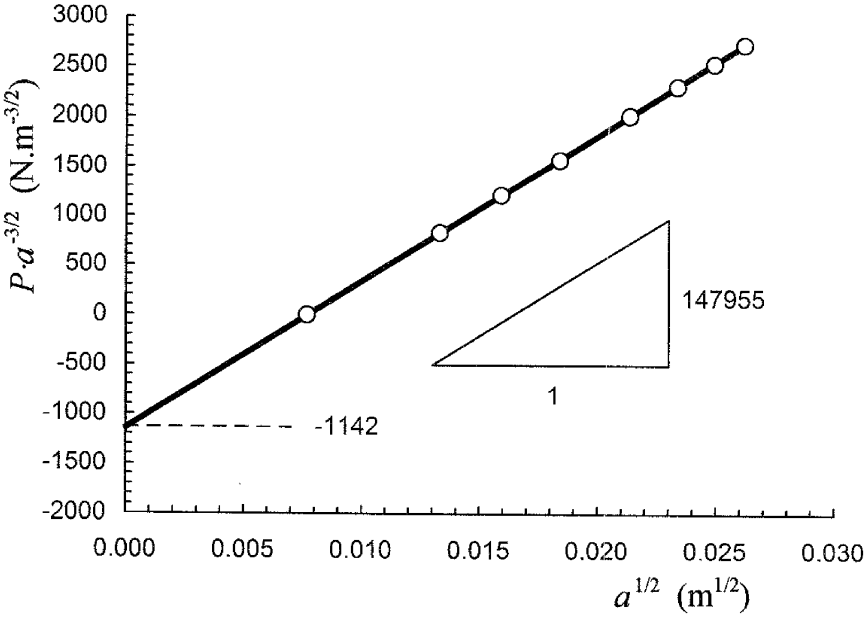

FIGURE 5 Parameter $P \cdot a^{-3/2}$ as a function of the square root of the radius a of the equilibrium contact area of the conical rigid punch (data from Figure 4). The slope of the rectilinear curve, equal to 147955 Pa, obtained from a linear regression on data points, allows one to assess the Young modulus, $E = 0.89\,\text{MPa}$ (assuming that Poisson's ratio $\nu = 0.5$). The y axis intersection value, equal to $-1142\ \text{N.m}^{-3/2}$, provides the Dupré energy of adhesion $w = 43\,\text{mJ.m}^{-2}$. (Reprinted after correction of misprints, from D. Vallet and M. Barquins, "Adhesive contact and kinetics of adherence of a rigid conical punch on an elastic half-space (natural rubber)," *Int. J. Adhesion and Adhesives* **22**, pp. 41–46, copyright 2002, with permission of Elsevier).

Experiments on the separation of the perfect conical punch were conducted starting with the same initial mass, $m_i = 5\,\text{gm}$, maintained for $t_i = 10\,\text{min}$, which corresponds to the force $P_i = 49\,\text{mN}$, when applying different active masses $m_a = -2, -1, -0.5, 0, 1, 2, 3$, and $4\,\text{gm}$. Figure 6 illustrates how the intensity of the active, mass, m_a, influences the evolution of the separation of the conical punch from the natural rubber surface. When $m_a = 0\,\text{gm}$, the contact area tends toward a new equilibrium with a decrease in the crack propagation speed, $V = -(1/2)\text{d}\varnothing/\text{d}t$. When $m_a < 0\,\text{gm}$, the evolution of the system leads to the rupture of the contact area. As expected it is observed that

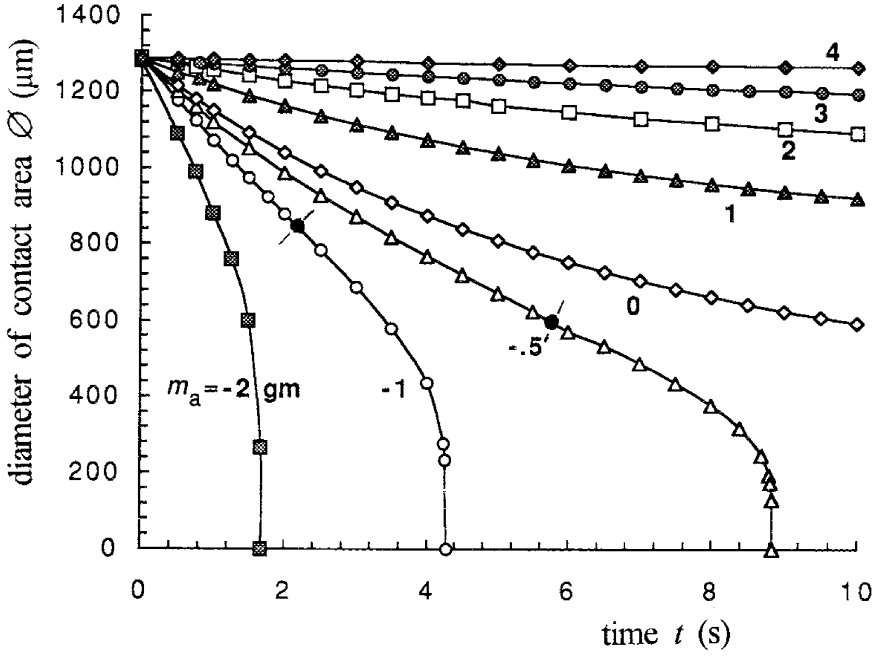

FIGURE 6 Kinetics of unloading: diameters, $\varnothing$, of the contact areas *versus* time, t, from the initial mass $m_i = 5\,\text{gm}$, applied on the conical punch for $t_i = 10\,\text{min}$, to various active masses $m_a = -2$, -1, -0.5, 0, 1, 2, 3, and 4 gm. The symbol ● corresponds to inflexion points.

the greater the tensile force associated with the load m_a, the earlier is the contact rupture.

Curves representing contact diameter, $\varnothing$, *versus* time t in Figure 6 and corresponding to active masses -0.5 and -1 gm clearly present inflexions, that is to say the crack first decelerates and then accelerates until contact is completely broken. At an inflexion point, the crack propagation speed, V, is minimum, and it is the same thing for the strain energy release rate, G, so the radius of contact corresponding to an inflexion point is obtained if the derivative $(\partial G/\partial A)_p$ at given load, P, is equal to zero. From Equation (5) with P_1 given by Equation (8), one can write [9]

$$\left(\frac{\partial G}{\partial A}\right)_p = \frac{1-\nu^2}{16\pi^2 \cdot E \cdot a^5} \cdot (P_1 - P) \cdot (P_1 + 3P). \tag{22}$$

The case $P = P_1$ has no physical meaning because it corresponds to a nonadhesive contact ($w = 0$). So, the radius of contact, a_{inf},

corresponding at an inflexion point on a curve $a(t)$ at constant negative load, P, is given by $P_1 = -3P$, and it is equal to

$$a_{\text{inf}} = \sqrt{\frac{-6P.(1-\nu^2)}{\pi \cdot E \cdot \tan\beta}}. \tag{23}$$

When the applied active separation force corresponds to the mass $m_a = -0.5\,\text{gm}$, Equation (23) gives the diameter $\varnothing_{\text{inf}(-0.5)} = 2a_{\text{inf}(-0.5)} = 600\,\mu\text{m}$, as is clearly shown in Figure 6. Likewise, with $m_a = -1\,\text{gm}$, the calculation provides $\varnothing_{\text{inf}(-1)} = 848\,\mu\text{m}$, a value which is in good agreement with the corresponding curve on Figure 6. Unfortunately, for $m_a = -2\,\text{gm}$, $\varnothing_{\text{inf}(-2)} = 1200\,\mu\text{m}$, this value cannot be seen on Figure 6, because it is close to the value of the initial contact diameter $\varnothing_i = 1284\,\mu\text{m}$.

In order to study the adherence kinetics as previously described [4–10, 19, 24], the strain energy release rate was calculated with the help of Equation (5) for each experimental point on the graph in Figure 6, the force P_1 was evaluated by Equation (8), and the crack propagation speed, $V = (1/2)\text{d}\varnothing/\text{d}t$, was deduced from the measured value of the local slope of the tangent of the curve $\varnothing(t)$ at the point under consideration. Curve A, corresponding to the lower symbols on the right-hand side in the Figure 7, presents the values calculated using the results from Figure 6. This curve tends towards the thermodynamic value $w = 43\,\text{mJ.m}^{-2}$.

EXPERIMENTAL RESULTS FOR THE FLAT-ENDED CONE AND DISCUSSION

Equilibrium and separation kinetics experiments were carried out at constant temperature, $\theta = 25^\circ\text{C}$, and relative humidity, $RH = 49\%$, between a truncated conical punch, made of Plexiglass® (PMMA), with the vertical half-angle $\beta = 5$ degrees (Figure 2), having a circular flat zone of diameter $\varnothing_{\text{flat}} = 2a_{\text{flat}} = 514\,\mu\text{m}$, and the smooth and flat surface of a sheet of the same soft unfilled vulcanized natural rubber (Young's modulus $E = 0.89\,\text{MPa}$, Poisson's ratio $\nu = 0.5$ and glass transition temperature $T_g = 201\,\text{K}$) with a thickness $e = 6\,\text{mm}$, as in previous experiments done with the perfect cone. The curve A in Figure 8 shows the equilibrium contact diameters, $\varnothing$, as a function of initial compressive masses, m_i.

Due to the intervention of molecular attraction forces of van der Waals type, a finite area of contact exists at zero applied load. Moreover, as is well known for spherical indenters, flat punches, flat-ended spheres, and cone [7, 9, 10–11, 19, 22–24], equilibrium

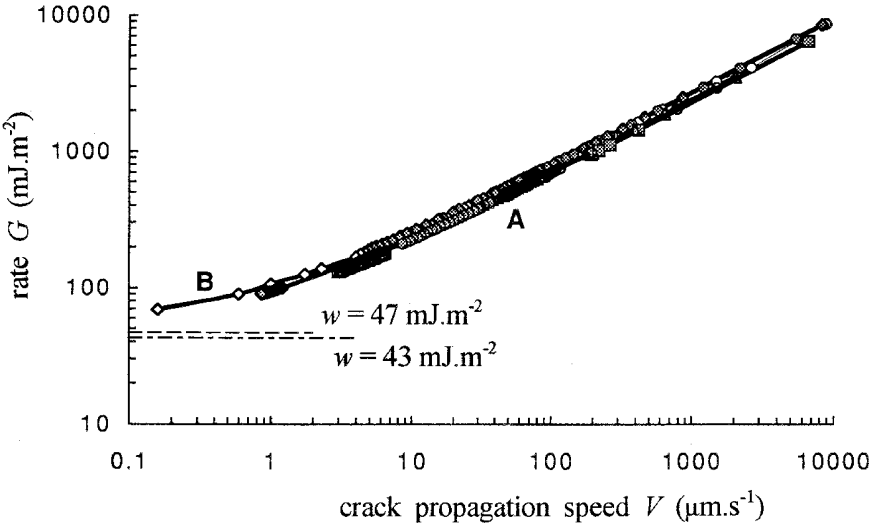

FIGURE 7 Strain energy release rates, G, *versus* crack propagation speed, $V = (1/2)\mathrm{d}\varnothing/\mathrm{d}t$. Curve A (lower symbols on the right-hand side): experimental data deduced from Figure 6, this curve tends towards the thermodynamic value $w = 43\,\mathrm{mJ.m^{-2}}$. Curve B (higher symbols on the left-hand side): experimental data deduced from Figure 8, this curve tends towards the new Dupré energy of adhesion $w = 47\,\mathrm{mJ.m^{-2}}$.

contact areas exist under negative loading (Figure 8, Curve A). For comparison, identical measures were found with the perfect cone used in the previous set of experiments (Figure 8, Curve B). It is very clear that in the case of contact with a perfect conical punch, the contact area with the rubber surface can support only very small tensile loads with regards to the case of a flat-ended cone.

Due to the slight variation of environmental conditions with regard to those observed in the previous set of experiments performed with the perfect cone, the equilibrium contact of this perfect cone was again studied in order to assess the new Dupré energy of adhesion with the help of the relation in Equation (13). The curve representing $P \cdot a^{-3/2}$ as a function of the square root of the contact radius $a = \varnothing/2$ was drawn as in Figure 4, and the ordinate at the origin is equal to $-\sqrt{(32/3)\pi \cdot E \cdot w} = -1884\,\mathrm{N.m^{-3/2}}$. The corresponding calculated value $w = 47\,\mathrm{mJ.m^{-2}}$ (using $E = .89\,\mathrm{MPa}$) is slightly greater than the previous one in the first set of experiments performed with the perfect cone due to the small decrease in relative humidity ($HR =$ 49% instead of 53%).

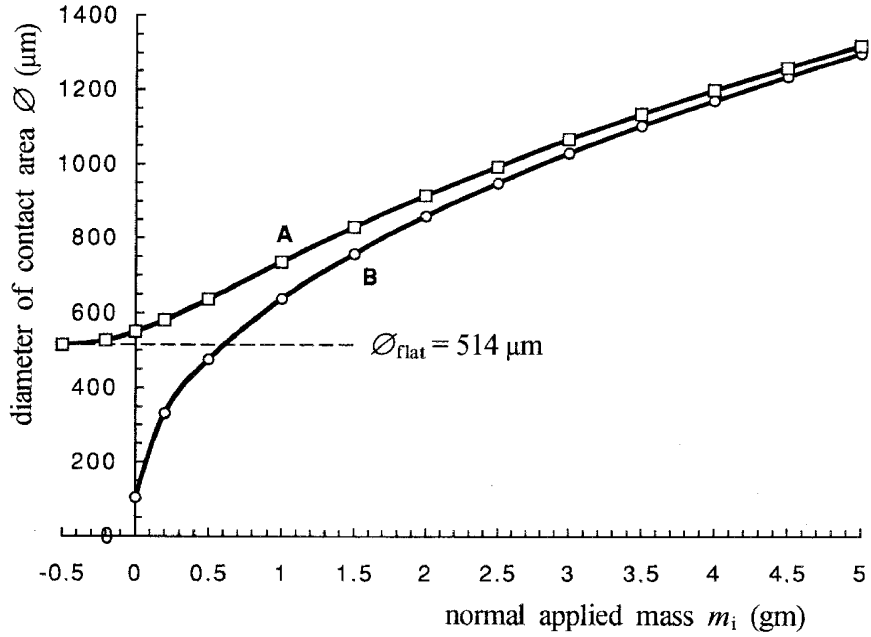

FIGURE 8 Diameter, $\varnothing$, of equilibrium contact areas between a truncated cone (flat zone of diameter $\varnothing_{flat} = 514\,\mu m$) and a perfect one, and the flat and smooth surface of an elastic solid (same unfilled natural rubber as previously used in cone study) as a function of the normal applied mass, m_i. The lines join experimental data (Curve A, truncated cone; Curve B, perfect conical punch).

Experiments on the separation of the flat-ended cone were conducted starting with the same initial mass $m_i = 5\,gm$, maintained for $t_i = 10\,min$, which corresponds to the force $P_i = 49\,mN$, when applying two different active masses $m_a = -0.6$ and $-1\,gm$. Figure 9 compares the evolution *versus* time of diameters of contact areas of the truncated cone (Curves A and A′) and the perfect one (Curves B and B′). It is clearly demonstrated how a flat zone can cancel or delay, following the intensity of the active mass, m_a, the rupture of the adhesive contact. As previously seen for a perfect conical punch (here Curves B and B′), it is observed that the greater the tensile force associated with the load m_a, the earlier the contact rupture. It can be pointed out that the part of the curve A′, for contact diameters smaller than $\varnothing_{flat} = 514\,\mu m$, obviously corresponds to the rupture of a cylindrical punch with a circular cross section [11].

In order to study the adherence kinetics, the strain energy release rate was calculated with the help of Equation (5) for each

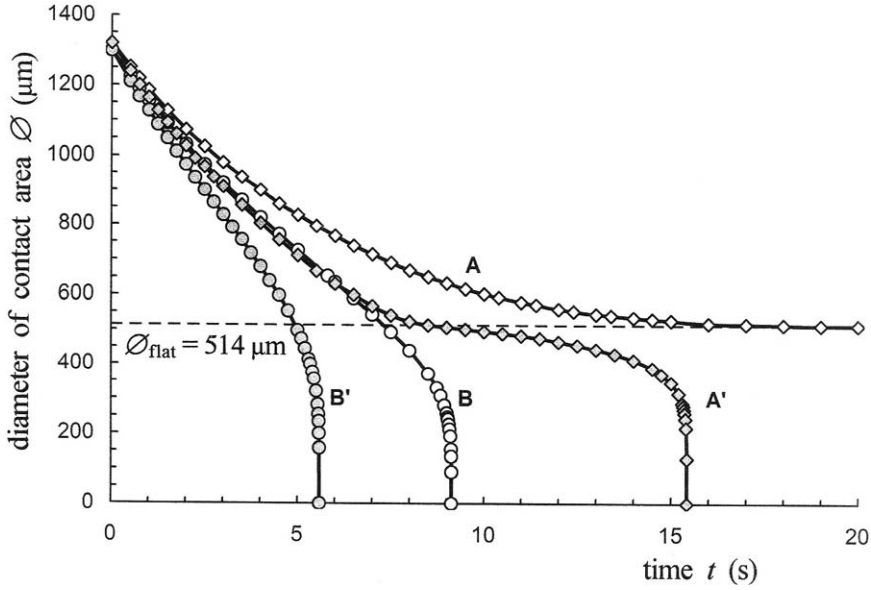

FIGURE 9 Kinetics of unloading: diameter, $\varnothing$, of the contact area *versus* time, t, from the initial mass $m_i = 5\,\text{gm}$, applied for $t_i = 10\,\text{min}$, to two active masses $m_a = -0.6$ and $-1\,\text{gm}$, for the flat-ended cone (Curves A and A′) and the perfect one (Curves B and B′). Curves A and B correspond to the applied mass $m_a = -0.6\,\text{gm}$, and Curves A′ and B′ correspond to the mass $m_a = -1\,\text{gm}$.

experimental point on the graph in Figure 9, the force P_1 was evaluated by Equation (16), and the crack propagation speed, $V = -(1/2)\mathrm{d}\varnothing/\mathrm{d}t$, was deduced from the measured value of the local slope of the tangent of the curve $\varnothing(t)$ at the point under consideration. The curve B on Figure 7 (higher symbols on the left-hand side) presents the values calculated using the results from Figure 9. This curve tends towards the thermodynamic value $w = 47\,\text{mJ.m}^{-2}$. As previously mentioned, one notes that whatever is the imposed separation force, $P_a = m_a \cdot g$, the points are found on the same graph $G(V)$, which proves that the evaluation of the Dupré adhesion energy is again correct.

The slight difference between Curve B and Curve A on Figure 7 is due to the small variation of environmental conditions between the two sets of experiments, especially concerning the relative humidity. It is clearly demonstrated here that, for a same value of the strain energy release rate, G (along a horizontal line on diagram $G(V)$ in Figure 7), the crack propagation speed, V, is slightly smaller (Curve B)

when the Dupré energy adhesion is increased ($w = 47\,\text{mJ.m}^{-2}$ instead of $43\,\text{mJ.m}^{-2}$), because the "motor" of the crack ($G-w$) is smaller.

Using the values of the graphs presented on Figure 7 and the values of w ($w = 47\,\text{mJ.m}^{-2}$ for data from Curve B and $w = 43\,\text{mJ.m}^{-2}$ for data from Curve A), Equation (20) allows one to draw the variation of the viscoelastic dissipation function, Φ, for our natural rubber sample as a function of the usual parameter $a_T \cdot V$, V being the crack propagation speed at the interface between the cone, the truncated cone, and the elastomer sample, and a_T, being the shift factor of the WLF transformation. In the first set of experiments the temperature $\theta = 26^\circ\text{C}$ corresponds to $a_T = 1.43 \cdot 10^{-3}$, whereas in the second one $\theta = 25^\circ\text{C}$ corresponds $a_T = 1.57 \cdot 10^{-3}$. Results are presented in Figure 10 for the reference temperature $\theta = 25^\circ\text{C}$.

Figure 10 regroups all the experimental data of the present study, which fall on the single master curve $\Phi = k \cdot (a_T \cdot V)^{0.55}$ (heavy straight line) with $k = 2520$ and the crack propagation speed, V, being valued using S.I. units. As expected for our rubber-like material,

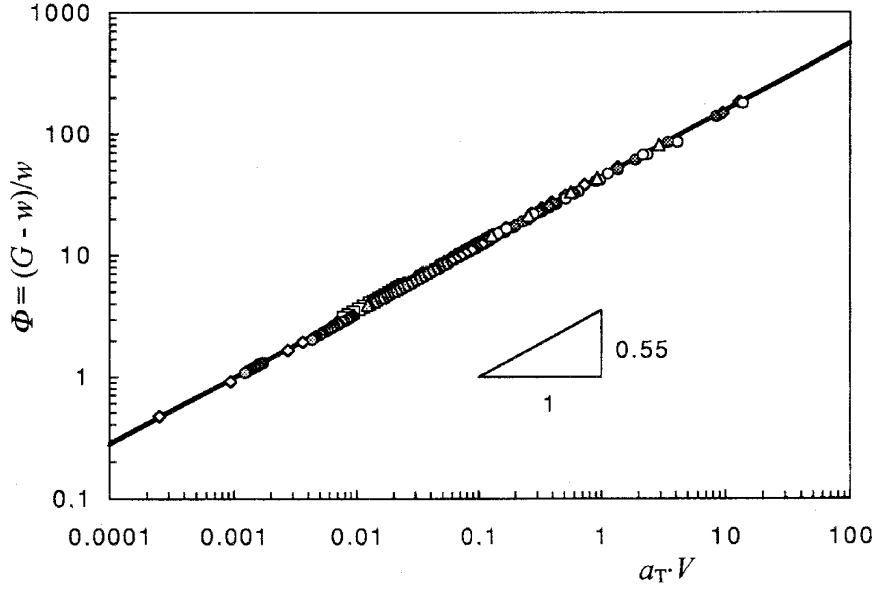

FIGURE 10 This master curve, which represents the dissipation function, Φ, *versus* the $a_T \cdot V$ parameter, regroups all the experimental data obtained in the present study. The heavy straight line shows $\Phi = k \cdot (a_T \cdot V)^{0.55}$, where $k = 2520$ and V are valued using S.I. units, and all the results fit with an accuracy of the order of 1%.

Figure 10 clearly illustrates that the function Φ varies as the power function $V^{0.55}$, for a fixed temperature, with a very good accuracy in the order of 1%.

CONCLUSION

The results of this study incontestably demonstrate and confirm that a single master curve can be drawn and that the variation $\Phi \sim V^{0.55}$ is characteristic of the propagation in Mode I at the interface of our rubber material (soft unfilled vulcanized natural rubber, characterized by Young's modulus $E = .89\,\text{MPa}$, Poisson's ratio $\nu = 0.5$, and glass-transition temperature $T_g = 201\,\text{K}$) in contact with a rigid and optically smooth axisymmetrical punch of convex arbitrary profile, as much as the viscoelastic losses remain confined to a very small volume surrounding the crack tip at the spot where the deformation speeds are high in such a way that the strain energy release rate, G, can be calculated by use of the theory of linear elasticity. Present results concerning the adherence of a perfectly axisymmetrical rigid cone and a truncated one, optically smooth, with the same half-angle, made of Plexiglass® (PMMA), lead to the proposition to write the dissipation function, Φ, as the product $\Phi = 2520 \cdot (a_T \cdot V)^{0.55}$, if the crack propagation speed V (equal to the variation with time of the radius of the contact area whose the limit can be seen as a crack tip) is valued in S.I. units, at the reference temperature $\theta = 25^\circ\text{C}$, with a quite good accuracy in the order of 1%.

REFERENCES

[1] Maugis, D., and Barquins, M., *C. R. Acad. Sci. Paris* **291**, 161–164 (1980).
[2] Sneddon, I. N., *Int. J. Engng. Sci.* **3**, 47–57 (1965).
[3] Barquins, M., and Maugis, D., *J. Méc. Théor. Appl.* **1**, 331–357 (1982).
[4] Barquins, M., and Charmet, J.-C., *J. Adhesion* **57**, 5–19 (1996).
[5] Charmet, J.-C., and Barquins, M., *Int. J. Adhesion Adhesives* **16**, 249–254 (1996).
[6] Robbe-Valloire, F., and Barquins, M., *Int. J. Adhesion Adhesives* **18**, 29–34 (1998).
[7] Robbe-Valloire, F., and Barquins, M., *Int. J. Adhesion Adhesives* **19**, 287–294 (1999).
[8] Charmet, J.-C., Vallet, D., and Barquins, M., *Microstructure and Microtribology of Polymer Surfaces* (Tsukruk and Wahl, Washington, DC, 2000), ASC Series 741, pp. 42–65.
[9] Vallet, D., and Barquins, M., *Int. J. Adhesion Adhesives* **22**, 41–46 (2002).
[10] Bouissou, S., and Barquins, M., *Int. J. Adhesion Adhesives* **22**, 459–463 (2002).
[11] Maugis, D., and Barquins, M., *J. Phys. D: Appl. Phys.* **11**, 1989–2023 (1978).
[12] Love, A. E. H., *Quart. J. Math. (Oxford)* **10**, 161–175 (1939).
[13] Maugis, D., and Barquins, M., *J. Phys. D: Appl. Phys.* **16**, 1843–1874 (1983).
[14] Barquins, M., *Wear and friction of elastomers* (Denton and Keshavan, Philadelphia, 1992), **ASTM STP 1145**, pp. 82–113.

[15] Gent, A. N., and Schultz, J., *J. Adhesion*. **3**, 281–294 (1972).
[16] Andrews, E. H., and Kinloch, A. J., *Proc. Roy. Soc. Lond. A*. **332**, 385–399 and 401–414 (1973).
[17] Williams, M. L., Landel, R. F., and Ferry, D., *J. Amer. Chem. Soc*. **77**, 3701–3707 (1955).
[18] Ramond, G., Pastor, M., Maugis, D., and Barquins, M., *Cahier G. F. R*. **6**, 67–89 (1985).
[19] Barquins, M., and Shanahan, M. E. R., *Int. J. Adhesion Adhesives* **17**, 313–317 (1997).
[20] Barquins, M., *J. Adhesion* **14**, 63–82 (1982).
[21] Roberts, A. D., and Othman, A. B., *Wear*. **42**, 119–133 (1977).
[22] Johnson, K. L., Kendall, K., and Roberts, A. D., *Proc. Roy. Soc. Lond. A*. **324**, 301–313 (1971).
[23] Barquins, M., *Int. J. Adhesion Adhesives* **3**, 71–84 (1983).
[24] Maugis, D., and Barquins, M., In *Adhesion and Adsorption of Polymers* (Lee, L.-H., (Ed.) Plenum, New York, 1980), pp. 203–277, Polymer Science and Technology, vol. 12A.